with Cu proteins. Therefore, presence of a countable N donor probably implicates presence of a histidine.

It has also been possible to get an ESR spectral match for species such as $Cu(en)(imH)_2^{2+}$ and $Cu(trien)(imH)^{2+}$ (having a pendant amine) by means of equivalent donor sets such as $Cu(his)_2^{2+}$ and $Cu(dien)(imH)^{2+}$. Therefore, the behaviors of various CuL_4^{2+} and CuL_5^{2+} donor sets are reasonably additive in terms of ESR parameters with simple monodentate plus simple chelate model assemblies. ^{63}Cu isotopic labeling has shown that both the ^{63}Cu and ^{65}Cu complexes exhibit equivalent N-shf couplings of 14 G.

The origin of the enhancement in the N-shf signal with the addition of an sp^2 N donor can be explained on the basis of the covalency of the bonding MO between Cu(II) and its σ donor ligands. The wave function for the bonding MO, ψ_b, can be written as a symmetry-adjusted linear combination (eq 1).[27] For a

$$\psi_b = a\, d_{x^2-y^2} + b\, d_{z^2} + C_1\, \sigma_{L_1} + C_2\, \sigma_{L_2} + \ldots + C_n\, \sigma_{L_n} \quad (1)$$

square-planar complex this is the B_{1g} MO with $b = 0$; $C_n = C_4$. The very weak coupling that is observed for $Cu(en)_2^{2+}$ or other all saturated N donors, combined with the observation of progressively stronger N-shf signals for $[CuN^*_4]^{2+} < [CuN^*_5]^{2+}$ species suggest that N-shf is observable only if the percentage of s character contributed by the nitrogen donors exceeds a critical value of 20.0% s. When all donors are sp^3, the detection level is borderline for N-shf coupling. However, if one or more ligands $L_1 \cdots L_n$ are of the sp^2 type, the percentage of N 2s character is increased in the resulting MO, ψ_b: 21% with one N* and three N donors up to 27% for four N* donors. In this manner the unpaired electron in a $d_{x^2-y^2}$ ground state (square planar or square pyramidal for Cu(II)) is brought into contact with all N centers to a greater degree by the addition of one or more ligands with a greater N 2s character. Since all are sp^2 donors for the $Cu(imR)_4^{2+}$ and $Cu(imR)_5^{2+}$ complexes, the percentage of N 2s component to ψ_b is maximized and the degree of N-shf is also maximized. This conceptual approach to explaining the effect of adding even just one N* donor to a complex which causes increased N-shf detectability has the additional attractive feature that all N donors will share approximately the same degree of contact with the unpaired electron via this MO as long as $|C_n|$ is nearly the same for each ligand. Therefore, all N donors will exhibit A_N of about the same value (14 G) unless the ligand's coefficient in ψ_b is very much less than any of the others due to structural changes. This latter point is rewarding in that for the $Cu(imCH_3)_6^{2+}$ species, formed at $x = 200$ $[imCH_3]:[Cu^{2+}]$ ratio, shows only strong N-shf for four of its in-plane donors; its coefficients for the axial donors C_5 and C_6 are very much smaller due to the Jahn–Teller distortion along the z axis.

There is a known theoretical basis for these results.[28] For frozen-solution spectra the measured value of A_N is the Fermi contact contribution (A_{FC}) to ligand superhyperfine coupling.[28] It is understood that A_{FC} is related to the s-orbital contribution α_s from which the % s character may be calculated (eq 2). As

$$A_{FC} = \frac{16\pi}{3}\gamma\beta\beta_N|\psi(0)|^2\alpha_s^2 \quad (2)$$

noted by Drago,[28] the existence and magnitude of A_N will be via the direct orbital coupling of the unpaired electron with the ligand through the MO in eq 1; spin polarization contributions are ignored. Indeed, the sp^3 donors are better candidates to exhibit stronger N-shf than the sp^2 ligands if spin polarization were important.

Acknowledgment. We express appreciation for support of this study under NSF Grant No. CHE 802183.

Supplementary Material Available: ESR spectra of Cu(II) complexes in Me_2SO/water glasses at 113 K (Figures 1sm–17sm) (7 pages). Ordering information is given on any current masthead page.

(27) Kivelson, D.; Nieman, R. *J. Chem. Phys.* **1961**, *35*, 149.

(28) Drago, R. S. *Physical Methods in Chemistry*; Saunders: Philadelphia, 1977; pp 488–487, and references therein.

(29) Diaz-Fleming, G.; Shepherd, R. E., submitted for publication in *Spectrochim. Acta, Part A*.

Contribution from the Corporate Research—Science Laboratories, Exxon Research and Engineering Company, Annandale, New Jersey 08801

Comparison of the Electronic Properties of $Mo_2O_2(\mu\text{-}S)_2(S_2)_2^{2-}$ and $Mo_2S_2(\mu\text{-}S)_2(S_2)_2^{2-}$

J. Bernholc*† and E. I. Stiefel*

Received April 22, 1985

A detailed theoretical analysis is presented of the similarities and differences of the electronic structures of $Mo_2O_2(\mu\text{-}S)_2(S_2)_2^{2-}$ (**1**) and $Mo_2S_2(\mu\text{-}S)_2(S_2)_2^{2-}$ (**2**). The analysis is based on self-consistent, first-principles electronic structure calculations for both systems. The replacement of the O atoms in **1** with S atoms in **2** leaves the higher filled MOs unaffected, although it removes the lower lying molecular orbitals corresponding to the Mo–O triple bond. The LUMOs, which in **1** are the Mo–O antibonding orbitals, are in **2** the Mo–S(terminal) antibonding orbitals at lower energies, decreasing the LUMO–HOMO gap in accordance with experimental observations. The energies of other antibonding orbitals are shifted somewhat to lower energies in going from **1** to **2**. The results suggest a similar reactivity pattern for reactions involving primarily the HOMO S_2 π^* orbitals, i.e., reactions with electrophiles. For reactions with nucleophilic components, somewhat lower activation energies should be expected due to the lowering of the HOMO–LUMO gap in **2** compared to that in **1**.

Introduction

The ions $Mo_2O_2(\mu\text{-}S)_2(S_2)_2^{2-}$ (**1**) and $Mo_2S_2(\mu\text{-}S)_2(S_2)_2^{2-}$ (**2**) belong to a large class of compounds that serve as models for active sites in molybdoenzymes[1] and in hydrodesulfurization and hydrodenitrogenation catalysts.[2] The isostructural ions consist of a formally $Mo_2O_xS_{4-x}^{2+}$ central core ($x = 2$ or 0) ligated by two S_2^{2-} diatomics (Figure 1).

$Mo_2O_2(\mu\text{-}S)_2(S_2)_2^{2-}$ was first synthesized in 1978 by thermal decomposition of $MoO_2S_2^{2-}$.[3] It reacts with activated acetylene in a highly unusual fashion by inserting the acetylene linkage into the terminal Mo–S linkage[4] to form a five-membered chelating

† Present address: Department of Physics, North Carolina State University, Box 8202, Raleigh, NC 27695.

(1) (a) Stiefel, E. I. In *Molybdenum and Molybdenum-Containing Enzymes*; Coughlan, M. P., Ed.; Pergamon: New York, 1980. (b) Spence, J. T. *Coord. Chem. Rev.* **1983**, *48*, 59. (c) Holm, R. H. *Chem. Soc. Rev.* **1981**, *10*, 454. (d) Averill, B. A. *Struct. Bonding (Berlin)* **1983**, *53*, 59. (e) Coucouvanis, D. *Acc. Chem. Res.* **1981**, *14*, 201.

(2) (a) Stiefel, E. I. Proceedings of the Climax Fourth International Conference on the Chemistry and Uses of Molybdenum; Barry, H. F., Mitchell, P. C. H., Ed.; Climax Molybdenum Co., Ann Arbor, MI, 1982. (b) Draganjac, M.; Simhon, E.; Chan, L. T.; Kanatzidis, M.; Baenziger, N. C.; Coucouvanis, D. *Inorg. Chem.* **1982**, *21*, 3322. (c) Miller, W. K.; Haltiwanger, R. C.; Van Derveer, M. C.; Rakowski DuBois, M. *Inorg. Chem.* **1983**, *22*, 2973 and references therein.

0020-1669/86/1325-3876$01.50/0

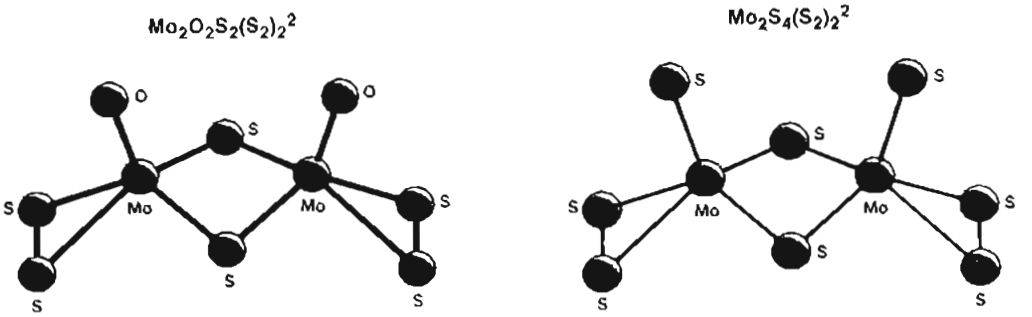

Figure 1. Perspective view of the $Mo_2O_2(\mu\text{-}S)_2(S_2)_2^{2-}$ and $Mo_2S_2(\mu\text{-}S)_2(S_2)_2^{2-}$ anions.

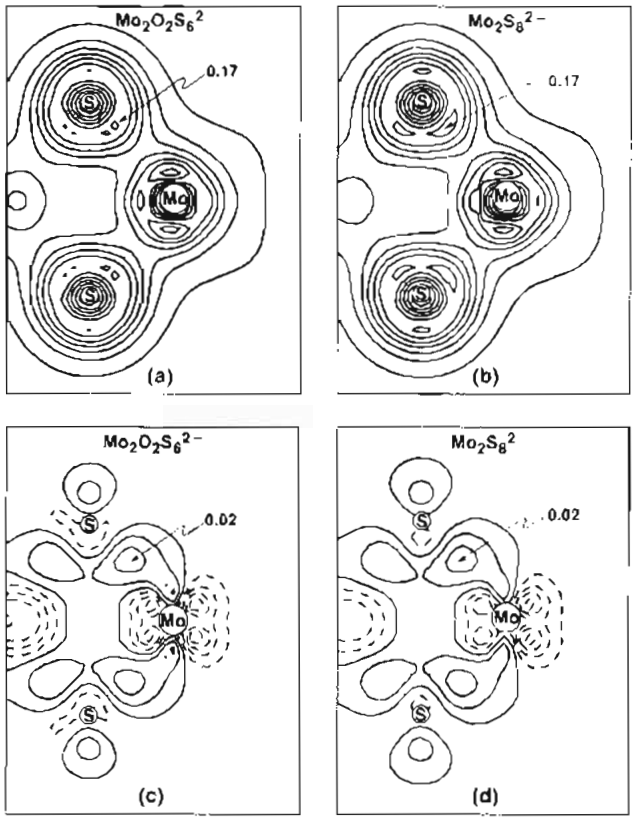

Figure 2. Contour maps of the charge density (a) in $Mo_2O_2(\mu\text{-}S)_2(S_2)_2^{2-}$ and (b) in $Mo_2S_2(\mu\text{-}S)_2(S_2)_2^{2-}$ and the differences between these charges and the superposition of charges of neutral atoms (c) in $Mo_2O_2(\mu\text{-}S)_2(S_2)_2^{2-}$ and (d) in $Mo_2S_2(\mu\text{-}S)_2(S_2)_2^{2-}$. The plotting plane contains one of the Mo atoms and the bridging S atoms. The contour levels are in atomic units, and the contour spacing is linear.

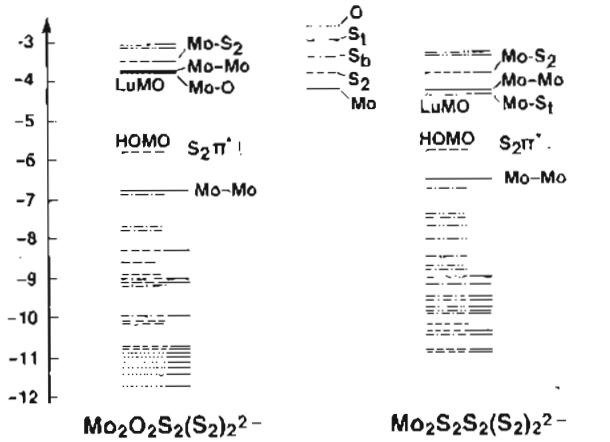

Figure 3. Energy level diagram for $Mo_2O_2(\mu\text{-}S)_2(S_2)_2^{2-}$ and $Mo_2S_2(\mu\text{-}S)_2(S_2)_2^{2-}$. The principal contribution of the ligands to each energy level is indicated in the figure. The dotted line denotes principally an oxygen level; the dashed-doubly dotted line, a terminal sulfur level; the dashed-dotted line, a bridging sulfur level; and a dashed line, a sulfur dimer level. An addition of a solid line after the level denotes a significant Mo admixture. Note that the HOMOs of the two molecules are at essentially the same energy (the energy level diagrams have *not* been aligned).

ring containing a vinyl disulfide ligand.

The $Mo_2S_2(\mu\text{-}S)_2(S_2)_2^{2-}$ ion was first prepared in 1983 by the redox reaction of MoS_4^{2-} with organic disulfides in solution.[5] The reaction follows a multistep pathway that involves induced internal electron transfer from sulfur to molybdenum.[6] In the following we will see that the electronic structure of **2** is sufficiently similar to that of **1** and that the S_2 and Mo–S_2 subunits should have similar reactivity patterns in the two complexes.

Previous theoretical calculations for transition-metal sulfides include a study of MoS_4^{2-},[7] of models of Fe–S clusters in proteins,[8] and of mononuclear Rh and Ir complexes ligated by a S_2^{2-} and four phosphine ligands.[9] In our own work we have carried out calculations for MoS_4^{2-} and $Mo_3S_9^{2-}$[10] and for $Mo_2O_2(\mu\text{-}S)_2(S_2)_2^{2-}$.[11]

Calculations

The electronic structure calculations were carried out by using first-principles pseudopotentials[12] (effective core potentials) to describe the core–valence interactions. In this way, only valence electrons enter the calculations, making treatments feasible even for large systems. The pseudopotentials were constructed from atomic calculations. They are parameter-free and reproduce exactly all-electron atomic properties.

The electron–electron interactions were included by the local density theory of electronic exchange and correlation.[13] This formalism includes correlation contributions derived from the theory of electron gas[13] while maintaining a simple molecular orbital description of effective one-electron wave functions. The analysis of the results is not more difficult than in the extended Hückel method[14] but the calculations are first principles and completely parameter-free.

The pseudo wave functions of each atom were expanded in Gaussian orbitals. Four Gaussian exponents were used for each principal quantum

(3) Müller, A.; Rittner, W.; Neumann, A.; Sharma, R. C. *Z. Anorg. Allg. Chem.* **1981**, *472*, 69.
(4) Halbert, T. R.; Pan, W.-H.; Stiefel, E. I. *J. Am. Chem. Soc.* **1984**, *105*, 5476.
(5) Pan, W.-H.; Harmer, M. A.; Halbert, T. R.; Stiefel, E. I. *J. Am. Chem. Soc.* **1984**, *106*, 459.
(6) Harmer, M. A.; Coyle, C.; Halbert, T. R.; Stiefel, E. I. to be submitted for publication.
(7) Kutzler, F. W.; Natoli, C. R.; Misemer, D. K.; Doniach, S.; Hodgson, K. O. *J. Chem. Phys.* **1980**, *73*, 3274.
(8) (a) Bair, R. A.; Goddard, W. A., III *J. Am. Chem. Soc.* **1978**, *100*, 5669. (b) Noodleman, L.; Baerends, E. J. *J. Am. Chem. Soc.* **1984**, *106*, 2316. (c) Geurts, P. J. M.; Gosselink, J. W.; Van Der Avoird, A.; Baerends, E. J.; Snijders, J. G. *Chem. Phys.* **1980**, *46*, 133. Aizman, A.; Case, D. A. *J. Am. Chem. Soc.* **1982**, *104*, 3269. Cook, M.; Karplus, M. *J. Am. Chem. Soc.* **1985**, *107*, 257; *J. Chem. Phys.* **1985**, *83*, 6344. Noodleman, L.; Norman, J. G., Jr.; Osborne, J. H.; Aizman, A.; Case, D. A. *J. Am. Chem. Soc.* **1985**, *107*, 3418.
(9) Ginsberg, A. P.; Osborne, J. H.; Sprinkle, C. R. *Inorg. Chem.* **1983**, *22*, 254.
(10) Bernholc, J.; Stiefel, E. I. *Inorg. Chem.* **1985**, *24*, 1323.
(11) Bernholc, J.; Holzwarth, N. A. W. *J. Chem. Phys.* **1984**, *81*, 3987.
(12) Kerker, G. *J. Phys. C: Solid State Phys.* **1980**, *13*, L189.
(13) (a) Hohenberg, P.; Kohn, W. *Phys. Rev.* **1964**, *136*, B864. (b) Kohn, W.; Sham, L. J. *Phys. Rev.* **1965**, *140*, A1133.
(14) Hoffman, R. *J. Chem. Phys.* **1963**, *39*, 1397.

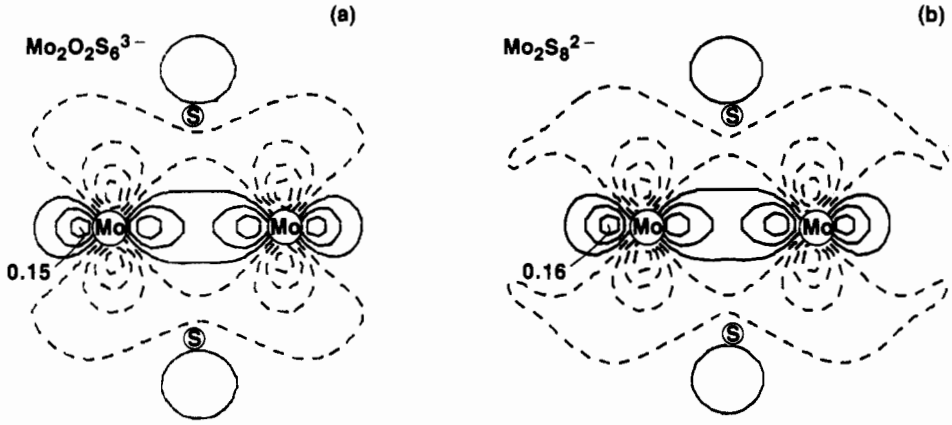

Figure 4. Contour maps of the Mo–Mo bond (a) in $Mo_2O_2(\mu\text{-}S)_2(S_2)_2^{2-}$ and (b) in $Mo_2S_2(\mu\text{-}S)_2(S_2)_2^{2-}$. The plotting plane contains the two Mo atoms. The projections of positions of the bridging sulfur atoms are also indicated.

number. The calculations started by superposition of atomic charge densities and were iterated to self-consistency. The self-consistency effects were found to be important for an accurate account of charge transfer. The details of the calculational procedure used in this work may be found in ref 11, together with values of the Gaussian exponents.

In the calculation of the absorption spectrum, we have used differences between ground-state eigenvalues as estimates of the transition-state energies. Since the molecular orbitals of Mo–S systems are quite delocalized, transition-state effects would change these results by less than 0.2 eV (cf. ref 10). In comparing the calculated values with experiment, one should keep in mind that the local density theory underestimates optical gaps by 25–30% in solids (see, for example, ref 15).

The electronic structure of $Mo_2O_2(\mu\text{-}S)_2(S_2)_2^{2-}$ has been described previously.[11] In this work, we compare it to that of $Mo_2S_2(\mu\text{-}S)_2(S_2)_2^{2-}$, with particular attention paid to orbitals around the HOMO–LUMO gap, which are important in the analysis of reactivity and spectra.

The atomic positions used in the calculations were obtained from published crystal structures (ref 16 and 5, respectively). Both molecules have approximately C_{2v} symmetry. Since the small deviations are likely to have been introduced by the constraints of crystal packing, we have used coordinates averaged to full C_{2v} symmetry. The energies of the molecular orbitals were quite insensitive to small variations in the atomic positions.

Results and Discussion

The changes in the overall bonding pattern are most readily apparent in a contour plot of the charge density. In Figure 2, we show contour plots of charge density for the two molecules. The plotting plane contains one of the two Mo atoms and the bridging sulfur atoms. Also shown are the contour maps of the difference between the molecular charge density and a superposition of charges of neutral atoms. It is evident from the figure that the bonding configuration remained largely unchanged upon substitution of O ligands for S ligands. Careful examination reveals that the charge increase in this plane is somewhat greater in **2** than in **1**, but the effect is minute. It is due to the greater electronegativity of the O ligand as compared to the S ligand.

It is also evident from the figure that the charge transfer from Mo to S is small (notice that the contour spacing and the charge density maximum in Figure 2b are 8 times smaller than in Figure 2a) and that most of the increase in the charge density is concentrated in the Mo–S bond region, attesting to a strong covalent component in Mo–S bonding. This is also true in other Mo–S systems, e.g., MoS_4^{2-} and $Mo_3S_9^{2-}$.[10]

The bonding of the S_2^{2-} ligands to the $Mo_2S_4^{2+}$ core follows a similar pattern, with a small charge transfer from Mo to S_2^{2-} and an increase in charge in the Mo–S_2 bond region, although somewhat closer to the sulfur atoms compared to above. The similarity of the charge contours of both molecules in the Mo–S_2 plane is as good as that in the plane of Figure 2. The substitution of O atoms for S atoms in the core has only had a very small effect on the bonding of S_2^{2-} ligands.

A more detailed picture of the bonding interactions is provided by the energy level diagram in Figure 3, which shows the valence molecular orbitals. The sulfur 3s and oxygen 2s derived levels do not show any net bonding effects and are not plotted. The principal orbital content for each level is indicated in the figure. These assignments are based on an analysis of contour maps of the individual levels and on a Mulliken population analysis for each level.

The lowest metal–ligand bonding levels in $Mo_2O_2(\mu\text{-}S)_2(S_2)_2^{2-}$ correspond to the approximately triply bonded Mo–O linkages. These are followed by two S_2–Mo bonding levels, S_2^{2-} 3p σ levels and an Mo–S(bridging) level. In $Mo_2S_2(\mu\text{-}S)_2(S_2)_2^{2-}$, the lowest levels are the S_2^{2-} 3p σ and π levels with a significant Mo admixture, followed by Mo–S(bridging) and Mo–S(terminal) bonding levels. The replacement of O atoms with S atoms in the core has not only removed the Mo–O levels and introduced higher lying Mo–S(terminal) levels but also significantly altered the energies and Mulliken populations of the remaining low-lying levels. This is due to the substantial delocalization of the molecular orbitals in Mo–S systems (see also ref 11 and 10).

The intermediate levels (between −9 and −7 eV) in both systems are the weakly bonding levels between distant sulfur atoms (at 3–3.5 Å), followed by nonbonding and finally weakly antibonding sulfur levels. The same general ordering of levels has been calculated for MoS_4^{2-} and $Mo_3S_9^{2-}$.[10]

The HOMOs in both molecules are the 3p π^* orbitals of the S_2^{2-} ligands. These orbitals lie in the plane perpendicular to the Mo–S_2 plane and do not contain any Mo admixture.[17] About 1 eV below the HOMOs is the single Mo–Mo bond (Figure 4). This bond is likely to be responsible for the short Mo–Mo distance of 2.82 Å and, in part, for the stability of the $MoO_xS_{4-x}^{2+}$ core.

Since the orbital content and the energies of the higher occupied orbitals are very similar in the two systems, the two molecules will appear very similar to electrophilic reagents.

The lowest unoccupied molecular orbitals involve the Mo–O and Mo–S(terminal) π^* orbitals, respectively. These are followed by an Mo–Mo 4d σ^* orbital and an antibonding orbital between the S_2^{2-} 3p π^* orbital in the Mo–S_2 plane and Mo 4d orbitals.

The HOMO–LUMO gap, calculated as the difference in orbital eigenvalues, is 2.0 eV in **1**, compared to 1.4 eV in **2**. This difference is mainly due to a much greater splitting between the Mo–O bonding and antibonding states, which bracket the Mo–S splittings. The energies of other antibonding orbitals in **1** are shifted upward compared to those in **2** due to delocalization of the individual states, which introduces small admixtures of Mo–O antibonding MOs into these orbitals.

When $Mo_2S_2(\mu\text{-}S)_2(S_2)_2^{2-}$ is compared with other Mo–S systems, like MoS_4^{2-} or $Mo_3S_9^{2-}$,[7,10] the level ordering follows the same general trends, i.e. the S 3s are the lowest valence levels but they are nonbonding. They are followed by Mo–S bonding levels

(15) Hamann, D. R. *Phys. Rev. Lett.* **1979**, *42*, 662.
(16) Clegg, W.; Mohan, N.; Müller, A.; Neumann, A.; Rittner, W.; Sheldrick, G. M. *Inorg. Chem.* **1980**, *19*, 2069.

(17) The S_2^{2-} 3p π^* orbitals in the Mo–S_2 plane have bonding interactions with the Mo 4d orbitals, which lower their energies.

and finally by nonbonding S 3p levels. The levels introduced by S_2^{2-} diatomics, however, retain their identity, and the interaction of the end S orbitals with the Mo levels is best described in terms of the σ and π MOs of the diatomics. The orbital character of these levels is similar to that studied in ref 9, where X_α calculations are reported for mononuclear Rh and Ir complexes ligated by a S_2^{2-} diatomic and four phosphine ligands. In our calculations, the single Mo–Mo bond lies 1 eV below the π^* levels of the diatomic.

The Mo–S systems differ significantly from nominally similar Fe–S systems,[8] since spin-polarization effects play a very important role in the latter case. For the "thiocubane" clusters[8c] both the HOMO and the LUMO consist mainly of spin-polarized Fe orbitals since both Fe(II) and Fe(III) are present in the ions, while the 1-Fe rubredoxin model[8a] and the Fe_2S_2 ferredoxin model[8b] have a sulfur-derived HOMO and an iron-derived LUMO.

The optical spectrum of $Mo_2O_2(\mu\text{-}S)_2(S_2)_2^{2-}$[3] shows transitions at 2.7 (21 800) and 3.35 (27 000) eV (cm^{-1}). The corresponding transitions for $Mo_2S_2(\mu\text{-}S)_2(S_2)_2^{2-}$[5] are at 2.16 (17 400) and 2.65 (21 400) eV (cm^{-1}). We assign the first transition to a charge-transfer excitation from the S_2^{2-} diatomics to the Mo–O and Mo–S_t antibonding orbitals (nominally Mo d orbitals), respectively. The second transition corresponds to a charge-transfer excitation from the bridging sulfur atoms to the same acceptor levels. Note that both the S_2^{2-} to Mo and bridging S to Mo charge-transfer bands are lower in energy than the terminal S→Mo charge-transfer bands. This is due to strong stabilization of S_t bonding levels by strong σ and π bonding with Mo. As mentioned in the previous section, optical transitions have been systematically underestimated by local density theory in solid-state applications. Since the optical transitions described above are between highly delocalized levels, similar effets are expected here. The calculated values are 2.0 and 3.0 eV for $Mo_2O_2(\mu\text{-}S)_2(S_2)_2^{2-}$ and 1.45 and 2.4 for $Mo_2S_2(\mu\text{-}S)_2(S_2)_2^{2-}$.

The reaction of $Mo_2O_2(\mu\text{-}S)_2(S_2)_2^{2-}$ with an activated acetylene,[4] such as dimethylacetylenedicarboxylate, involves insertion of two carbon atoms into one of the Mo–S_2 bonds. This reaction may involve nucleophilic attack of S on C with filled S levels interacting with low-lying empty levels (π^*) on the activated acetylene. It is noteworthy that the site of acetylene reactivity corresponds to the HOMO of **1**. Since the highest lying occupied orbitals in the S analogue, **2**, are very similar, a similar reactivity is expected. Moreover, the reaction may also involve the Mo–S_2 antibonding orbitals, perhaps in a second step. Since the Mo–S_2 antibonding orbital is shifted down in energy in **2** compared to the case of **1**, reactions with $Mo_2S_2(\mu\text{-}S)_2(S_2)_2^{2-}$ that have such a nucleophilic component could have a lower activation energy. Such arguments, however, depend upon detailed mechanisms of the acetylene reactions, which are under experimental study.

Summary

We have carried out a detailed analysis of the differences and similarities between the electronic properties of $Mo_2O_2(\mu\text{-}S)_2(S_2)_2^{2-}$ and $Mo_2S_2(\mu\text{-}S)_2(S_2)_2^{2-}$. We find that the replacement of oxygen atoms by sulfur atoms in the $Mo_2O_2S_2^{2+}$ core does not significantly affect the binding of S_2^{2-} to the core or the binding of the bridging sulfur atoms to the molybdenum atoms within the core. In particular, the S_2^{2-} π^* orbitals in the plane perpendicular to the Mo–S_2 bond remain the HOMOs in $Mo_2S_2(\mu\text{-}S)_2(S_2)_2^{2-}$. Their energies, as well as the energy and the orbital content in the single Mo–Mo bond, 1 eV below the HOMOs, are not significantly affected. For the unoccupied orbitals, the Mo–O π^* orbitals are replaced by Mo–S(terminal) π^* orbitals as the LUMOs. The invariance of the higher lying occupied orbitals and the relatively small changes in the unoccupied orbitals suggest an essentially similar reactivity pattern for $Mo_2S_2(\mu\text{-}S)_2(S_2)_2^{2-}$ toward simple electrophlic reagents. The lowering of the HOMO–LUMO gap, however, suggests a possible lowering of the activation energy for reactions involving the unoccupied orbitals. The results of these calculations together with mechanistic studies currently in progress lead to a better appreciation of reaction pathways available to molybdenum–sulfur systems.

Acknowledgment. It is a pleasure to thank Drs. T. R. Halbert, S. Harris, and W.-H. Pan for useful discussions.

Registry No. **1**, 73557-91-2; **2**, 88303-91-7.

Contribution from the Department of Chemistry, University of the Witwatersrand, Johannesburg, South Africa

Control of Metal Ion Selectivity in Ligands Containing Neutral Oxygen and Pyridyl Groups

Kirty V. Damu, M. Salim Shaikjee, Joseph P. Michael, Arthur S. Howard, and Robert D. Hancock*

Received January 6, 1986

The stabilities of the complexes of the ligand $(py)_2$-18-aneN_2O_4 (*N,N'*-bis(*o*-pyridylmethyl)-1,4,10,13-tetraoxa-7,16-diazacyclooctadecane) at 25 °C in 0.1 M $NaNO_3$ are reported, as well as those of DHEAMP (((bis(2-hydroxyethyl)amino)methyl)-pyridine), with a variety of metal ions. The log K_1 values for the $(py)_2$-18-aneN_2O_4 complexes are as follows: Cu^{2+}, 13.55; Ni^{2+}, 8.80; Zn^{2+}, 6.96; Cd^{2+}, 10.96; Ca^{2+}, 3.63; La^{3+}, 3.53; Sr^{2+}, 4.87; Pb^{2+}, 11.67; Ba^{2+}, 4.99. The constants for the protonation equilibria were, for $H^+ + L = HL^+$, log K = 7.44, for $H^+ + HL^+ = H_2L^{2+}$, log K = 6.26, and for $H^+ + H_2L^{2+} = H_3L^{3+}$, log K = 1.38. For DHEAMP, log K values are as follows: Cu^{2+}, 9.2; Ni^{2+}, 7.34; Zn^{2+}, 5.25; Ca^{2+}, 1.0; La^{3+}, 1.95; Pb^{2+}, 5.43. The protonation equilibria for DHEAMP were, for $H^+ + L = HL^+$, log K = 6.92, and for $H^+ + HL^+ = H_2L^{2+}$, log K = 1.16. The coordinating properties of ligands with neutral oxygen donors are discussed, and the suitability of $(py)_2$-18-aneN_2O_4 as a reagent for the treatment of lead poisoning is considered. The control of metal ion selectivity based on metal ion size is discussed, as well as the coordinating properties of ligands based on the 18-aneN_2O_4 ring, which have pendant donor groups attached to the nitrogens of the macrocyclic ring.

The metals lead, cadmium, and mercury are currently of environmental concern.[1] At present, none of the ligands used for removing these metal ions from the body in cases of metal poisoning can be regarded as very satisfactory.[1] Lead poisoning, which is our interest here, is treated with EDTA (see Figure 1 for structures of ligands), which has the drawback[1] of a lead/zinc selectivity of only 1.6 log units,[2] which means that excessive amounts of zinc are removed from the body during treatment. A further problem with EDTA is its relatively high affinity for

(1) May, P. M.; Bulman, R. A. *Prog. Med. Chem.* **1983**, *20*, 226.

(2) All formation constants referred to in this work, unless otherwise indicated, are from: Martell, A. E.; Smith, R. M. *Critical Stability Constants*; Plenum: New York, 1974–1977, 1979; Vol. 1–5. Where selectivities for one metal ion over another are indicated, the numerical value for the selectivity is simply the logarithm of the formation constant, log K, for the first metal ion minus log K for the second metal ion with the same ligand.

0020-1669/86/1325-3879$01.50/0